J Mater Sci (2008) 43:702–708
DOI 10.1007/s10853-007-2193-6

Ethylene vinyl acetate/expanded graphite nanocomposites by solution intercalation: preparation, characterization and properties

Jinu Jacob George · Anil K. Bhowmick

Received: 1 January 2007 / Accepted: 26 September 2007 / Published online: 31 October 2007

Abstract Nanodimensional reinforcing agents are introduced to polymer matrices to improve properties at very low loading. Natural graphite (NG) as such is not reinforcing in nature. But when modified to expanded graphite (EG) by high temperature heat treatment, this may be used as reinforcing nanofiller. In the present study, ethylene vinyl acetate (EVA) was reinforced with EG by solution intercalation, and the composite properties were compared with those of the virgin polymer and NG filled composite. The tensile strength exhibited an improvement of 35% with 4 wt% EG addition, while the modulus at 100% elongation was increased by 150% with respect to the control EVA. Another interesting feature was that unlike the conventional fillers, addition of EG did not reduce the elongation at break, due to the lubricating action of graphite. However, at a high loading of 8 wt%, the tensile strength showed a lower value, due to the agglomeration of graphite platelets. The storage modulus also showed increment with the addition of graphite without much change in the glass transition temperature. In addition to these, the EVA-EG nanocomposites exhibited high thermal conductivity and thermal degradation stability as compared to the virgin polymer. About 4 wt% of EG shifted the temperature of maximum rate of degradation by 14 °C towards higher temperature. These results were well supported by the swelling and morphological studies. The NG filled composite exhibited inferior properties to EVA-EG nanocomposites.

J. J. George · A. K. Bhowmick (✉)
Rubber Technology Centre, Indian Institute of Technology, Kharagpur 721302, India
e-mail: anilkb@rtc.iitkgp.ernet.in

Introduction

Incorporation of fillers in a polymer matrix gives rise to a new class of materials known as polymer composites, which have better potential for many applications. The interaction between a polymer and filler particles, when the size of the filler is 10^{-9} m at least in one dimension, leads to polymeric nanocomposites. Polymeric nanocomposites have been a topic of great interest for the last two decades for scientists all over the world. Numerous researchers have already reported the effect of different nanofillers like clay, carbon nanotubes and silica on polymer properties [1–5]. Development of nanocomposites from various clay and silica fillers and nanotubes has been discussed in several publications from our laboratory [6–11]. Also, a preliminary investigation on modified graphite based nanocomposite has been done [12].

Clay is a two dimensional plate like filler, which can impart high mechanical, barrier and other properties to a polymer. Graphite is also having the similar planar structure with several characteristics. If graphite could be dispersed in polymer matrix in the nanosize range, it can improve overall properties of the system. In addition, it can provide its own characteristic properties of thermal and electrical conductivity as well.

Graphite is an allotrope of carbon, the structure of which consists of graphene layers stacked along the c-axis in a staggered array [13]. It is a layered material, consisting of a structure where carbon atoms are bound by covalent bonds to other carbons in the same plane and only van der Waals forces are acting between successive layers. Since the van der Waals forces are relatively weak, it is possible for a wide range of atoms, molecules and ions to intercalate between graphite sheets [14]. The natural graphite (NG) as such is not reinforcing in nature. But when modified to expanded

graphite by high temperature heat treatment, this could be used as reinforcing nanofiller in various polymer matrices.

The exfoliation of graphite is a process, in which graphite expands along the c-axis, resulting in a puffed-up material with a low density and a high temperature resistance [15]. The effective method of preparing the expanded graphite is by rapidly heating the pre-treated graphite to a high temperature.

A few studies have been done on the effect of expanded graphite in various polymer matrices. Most of the studies were done on thermoplastic matrices like polystyrene, polymethyl methacrylate, polyvinyl alcohol and so on [16–18]. In the present study, we report the effect of expanded graphite on various properties of ethylene vinyl acetate (EVA). The elastomer EVA was selected because of its commercial importance and also of its wide range of applications in various fields.

Experimental

Materials

Rubber grade ethylene vinyl acetate (EVA) with 60% vinyl acetate content was supplied by Bayer (now Lanxess), Germany. The expanded graphite was supplied by Asbury Graphite Mills Inc, United States. The cross-linker for the rubber, dicumyl peroxide (DCP, 99% pure) was obtained from Hercules, India. Triallyl cyanurate (TAC), the co-crosslinker was procured from Fluka A G, Germany. Tetrahydrofuran (THF) of LR grade, used as the solvent for EVA was obtained from MERCK (India) Ltd., Mumbai, India.

Preparation of nanocomposites

The nanocomposites were synthesized by using a solution-mixing technique. EVA (5 g per batch) was dissolved in 50 ml of THF to make 10% solution of the rubber using a mechanical stirrer. 0.05 g of DCP as the curing agent and 0.05 g of TAC as the co-agent were added to the rubber solution. The solution was thoroughly stirred using a mechanical stirrer. The expanded graphite sample dispersed in THF was first sonicated for 15 min, and subsequently added to the rubber solution, while stirring at room temperature (27 °C). The final solution was cast over teflon trays and kept for air drying followed by vacuum drying at 50 °C till there was practically no weight variation. The dried films were molded in a hot press at a pressure of 5 MPa at 150 °C for an optimum cure time of 25 min, determined from a Monsanto oscillating disc rheometer (ODR, 100 S).

Methods

The particle size and surface area of the different graphite samples were measured using a Malvern-3601 (UK) particle size analyzer.

The X-ray diffraction studies were done using a Rigaku CN 2005 X-Ray Diffractometer, model: Miniflex (30 kV, 10 mA) with a Cu target (CuK_{α} radiation with $\lambda = 0.154$ nm) in the range of $2\theta = 10–50°$. The corresponding d-spacing of the powder graphite particles was calculated using the Bragg's Equation [19].

$$n\lambda = 2dSin\theta \quad (1)$$

where, λ is the wavelength of X-rays, d is the inter-planar distance and θ is the angle of incidence of the radiation.

The crystallite size within the graphite powders before and after modification was determined from the X-ray diffraction data using the following equation: [19, 20]

$$C_s = \frac{0.9\lambda}{\beta Cos\theta} \quad (2)$$

where, C_s is the crystallite size, λ is the wavelength of the incident X-ray beam, β is the full width at half maximum (FWHM) of the X-ray diffraction peaks and θ s the half of the angle 2θ corresponding to the peak.

The samples for TEM analysis were prepared by ultra-cryomicrotomy using a Leica Ultracut UCT. Freshly sharpened glass knives with cutting edge of 45° were used to get the cryosections of 50–70 nm thickness. Since these samples were elastomeric in nature, the temperature during ultra cryomicrotomy was kept at –50 °C (which was well below glass transition temperatures of EVA). The cryosections were collected individually on sucrose solution and directly supported on a copper grid of 300-mesh size. The microscopy was performed using a JEOL JEM-2010 (Japan) high resolution transmission electron microscope, operating at an accelerating voltage of 200 KV.

The mechanical properties of the composites were evaluated by a universal testing machine (UTM, Zwick 1445) on dumbbell specimens, punched out from the cast films using an ASTM Die C. All the tests were carried out as per ASTM D 412–99 method at 25 ± 2 °C, at a cross-head speed of 500 mm/min. The average values of three tests for tensile strength, tensile modulus and elongation at break are reported for each sample.

Dynamic mechanical thermal characteristics of the composite films (0.4–0.6 mm thick) were evaluated by using a DMTA IV (Rheometric Scientific) under tension mode. All the data were analysed using RSI Orchestrator application software on an ACER computer attached to the machine. The temperature sweep measurements were made over the range of temperatures from –35 °C to 20 °C. The

experiments were carried out at a frequency of 1 Hz at a heating rate of 2 °C/min. The storage modulus (E′) and the loss tangent (tan δ) data were recorded for all the samples under identical conditions.

The swelling studies of the rubber specimens were carried out in toluene at ambient condition (27 °C) for 72 h. Volume fraction of rubber, V_r, was calculated using the following equation [21, 22].

$$V_r = \frac{(D - FT)\rho_r^{-1}}{(D - FT)\rho_r^{-1} + A_0\rho_s^{-1}} \quad (3)$$

where, V_r is volume fraction of rubber in the swollen gel; D, the de-swollen weight of the composites; F, the fraction insoluble; T, the initial weight of the sample and A_0, the amount of solvent imbibed. ρ_r is the density of the rubber, while ρ_s is the density of the swelling solvent.

Polymer–filler interaction in the vulcanisates was examined using Kraus equation [23]

$$\frac{Vr_0}{Vr_f} = 1 - m\left(\frac{\phi}{1-\phi}\right) \quad (4)$$

where Vr_f is the volume fraction of rubber in the filled vulcanisate, ϕ is the volume fraction of filler in the filled vulcanisate and m is the slope of linear fit of the Kraus plot

The overall reinforcing behaviour of the filled system can be analysed by plotting Vr_0/Vr_f against $\phi/1-\phi$.

The slope of the resulting straight line gives a description of the reinforcement of the filler in that particular matrix.

The thermal conductivity of the various composite samples was measured as per ASTM C177. The thermal conductivity was calculated using the equation

$$K = \frac{Wt}{AdT} \quad (5)$$

where W is the power in Watts (here 4 W); K, the thermal conductivity; t, the thickness of sample; A, the area of the sample and dT, the stabilized temperature difference between the two plates where the sample is placed.

Thermal stability of the composites was investigated by thermo gravimetric analysis (TGA) by using a Perkin Elmer TGA instrument [Model: Pyris Diamond TG/DTA] from ambient to 800 °C at a programmed heating rate of 20 °C/min in nitrogen. A sample weight of approximately 10 mg was taken for all the measurements. The weight loss against temperature was recorded. Differential thermo gravimetric analysis (DTG) of the composites was represented in terms of the first derivative plots of the TGA curves. The data points denote the weight loss/time against temperature at the specified heating rate.

Table 1 Particle size and X-ray diffraction data of natural and expanded graphite samples

Sample	Particle size (μm)	Surface area (m^2/cc)	2θ (°)	d (nm)	Crystallite size (nm)
NG	67.62	0.15	28.6	0.31	48.3
EG	21.87	0.32	26.4	0.34	12.9

Results and discussion

Table 1 compares the particle size and the surface area of the expanded graphite with those of the NG. The smaller particle size, and hence higher surface area are due to the high temperature treatment to produce expanded graphite. The high temperature treatment causes the graphite layers to separate, and also to some extent destroy the crystalline structure. This greater surface area of the expanded graphite is advantageous in the making of nanocomposite, as it can lead to higher interaction between the platelets and the polymer molecules.

Figure 1 depicts the X-ray diffractogram of expanded graphite along with that of NG. A characteristic peak is observed for NG at 28.6°. The high sharpness indicates the high crystalline nature of the graphite, and corresponds to the diffraction from (002) plane. For the expanded graphite, the same 002 peak is observed at a slightly lower angle (26.4°) (Fig. 1, Table 1). This indicates that there is a higher interlayer spacing between the graphite platelets (0.34 nm vs. 0.31 nm). There is also a peak at 9.6° for the NG, which is almost absent in the case of expanded graphite (EG). The crystallite size is lower for the expanded graphite (Table 1). Figure 1 also depicts the X-ray

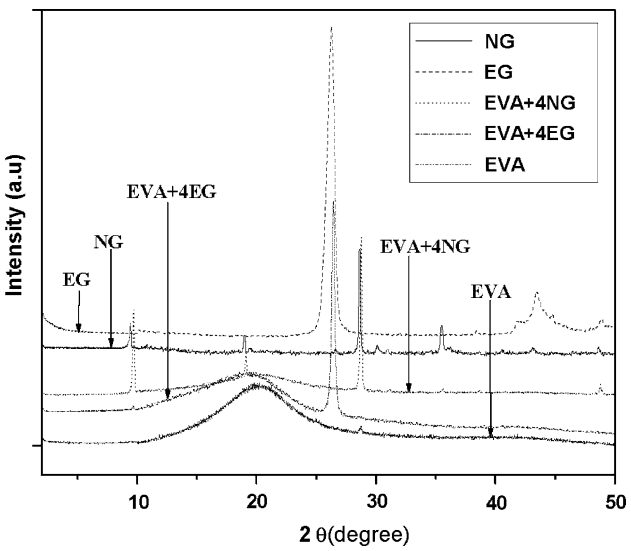

Fig. 1 X-ray diffractograms of NG, EG, EVA, EVA + 4EG and EVA + 4NG

diffraction patterns of neat EVA along with its composites, EVA-4EG and EVA-4NG. The hallow is due to the amorphous polymer portion. Also, the intensity of the graphite characteristic peak reduces and few other peaks disappear due to increase in amorphousness in the case of EVA-4EG. The sharp reflection at $2\theta = 26.4°$ is once again observed, which implies that the individual graphite nanosheets consist of multilayer graphite sheets with a d-spacing of 0.34 nm. Intrusion of polymer molecules does not change the nanostructure of graphite, and hence its crystal structure is retained. Similar observations were reported by Zheng et al. and Yasmin et al. [22, 23]

Figure 2a–c depicts the TEM pictures of the EVA-EG nanocomposites at 4 and 8 phr expanded graphite loading along with that of EVA-4NG. It is clear from Fig. 2a that graphite platelets are finely dispersed in the rubber matrix leading to higher interaction between the matrix and the filler particles. This again leads to better mechanical and dynamic mechanical properties (discussed later). The thickness of platelets is observed to be in the range of 20–30 nm, whereas at higher loading (8 phr), the graphite particles exhibit an agglomeration tendency (Fig. 2b), leading to poor overall properties for the composites prepared. The agglomerates exist in the thickness range of 80–120 nm. Similarly, EVA-4NG also exhibits clear agglomerations with an average thickness more than 100 nm.

Table 2 reports in-detail mechanical properties of the cured EVA-EG nanocomposites in terms of tensile modulus (at 50,100 and 200% elongations), tensile strength and elongation at break values. The values are calculated from the stress–strain curves, shown in Fig. 3. With increasing concentrations of the EG, the modulus of EVA increases. A maximum of around 35% increment in the tensile strength, with reference to the virgin EVA are attained. Although the tensile strength and modulus increase, the elongation at break does not decrease in the present system except for 8 phr filler. The increased elongation at break with the loading of graphite is possibly due to the slippage of the rubber chains over the fibrillar EG platelets, imparting some plasticizing effects within the system. But with 8 phr of filler, maximum strength is marginally reduced and also the elongation at break shows significant decrement, which may be due to agglomeration of EG within the rubber matrix. But the modulus exhibits increasing trend with the amount of EG, showing the dominant contribution of the filler particles to the ultimate modulus of the composite. The addition of NG adversely affects the tensile properties of the EVA due to poor dispersion of the filler particles leading to weak points.

Figure 4a–b represents the plots of dynamic storage modulus (Fig. 4a, in log scale) and the loss tangent against temperature (Fig. 4b) for the nanocomposites. The experimental temperature ranges from –35 °C to +20 °C. In the

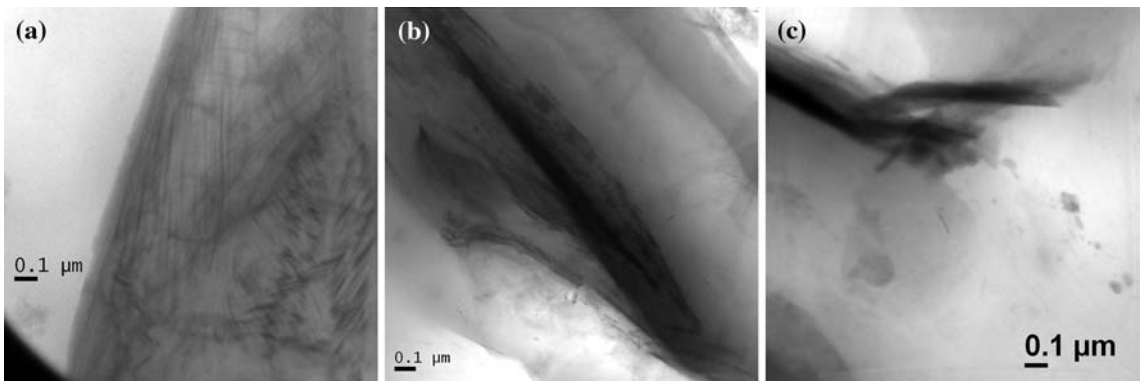

Fig. 2 TEM pictures of (**a**) EVA + 4EG (**b**) EVA + 8EG and (**c**) EVA + 4NG

Table 2 Tensile properties of EVA + EG nanocomposites and EVA + 4NG

Sample	Tensile strength (MPa)	Elongation at break (%)	Modulus (MPa) at		
			50%	100%	200%
EVA	5.54 ± 0.10	310 ± 10	0.72 ± 0.08	1.10 ± 0.10	2.70 ± 0.07
EVA + 1EG	6.03 ± 0.14	350 ± 10	0.76 ± 0.10	1.18 ± 0.12	2.82 ± 0.11
EVA + 2EG	6.58 ± 0.15	360 ± 10	0.95 ± 0.08	1.54 ± 0.09	3.44 ± 0.07
EVA + 4EG	7.51 ± 0.12	320 ± 10	1.26 ± 0.12	2.05 ± 0.10	4.14 ± 0.10
EVA + 8EG	4.86 ± 0.10	210 ± 10	1.74 ± 0.10	2.74 ± 0.11	4.67 ± 0.10
EVA + 4NG	4.59 ± 0.20	310 ± 10	0.66 ± 0.05	0.94 ± 0.05	1.68 ± 0.10

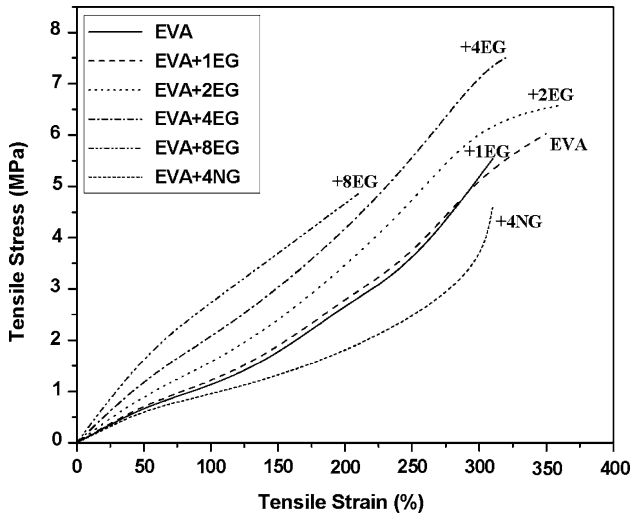

Fig. 3 Tensile stress versus strain plots of various EVA + EG nanocomposites along with that of EVA + 4NG

glassy region, the moduli show steady increase from the virgin rubber with the concentration of EG. A similar trend exists in the transition region also. The values of storage modulus and tan δ, at the representative temperatures are reported in Table 3. The increase in storage modulus with 4 phr of expanded graphite is significant at 20 °C, in line with the study of the tensile properties. Figure 4b demonstrates a slight reduction in the peak height with increase in the amount of graphite. A steady shift in the tan δ_{max}, which indicates the T_g of the system, towards higher temperature as a result of addition of EG is also noted up to 4 phr. But for 8 phr of EG, the T_g is found to be lower than that containing 4 phr EG. This may be due to the presence of agglomeration of graphite particles within the matrix (as shown earlier). This effect is very similar to the addition of carbon black, as reinforcing filler [24]. This may also be due to slippage of the chains over graphite layers. The EVA-NG composite exhibits only a slight increment in storage modulus with respect to the virgin elastomer, and the value of T_g and the modulus clearly indicate insignificant interaction with the matrix.

The results of mechanical and dynamic mechanical properties are well supported by the solvent swelling study of the various nanocomposites. More the volume fraction of rubber entrapped in the swollen gel, higher is the cross-link density. The gel formation increases with the amount of expanded graphite added to the matrix (Table 4) and therefore, it shows increased volume fraction of rubber, supporting the increase in modulus values obtained in mechanical and dynamic mechanical studies. This indicates the higher interaction between the filler and the polymer molecules due to the higher surface area of the nanofillers (Table 4). EVA-NG displays lower value of V_r, as compared to the counterpart EVA-EG.

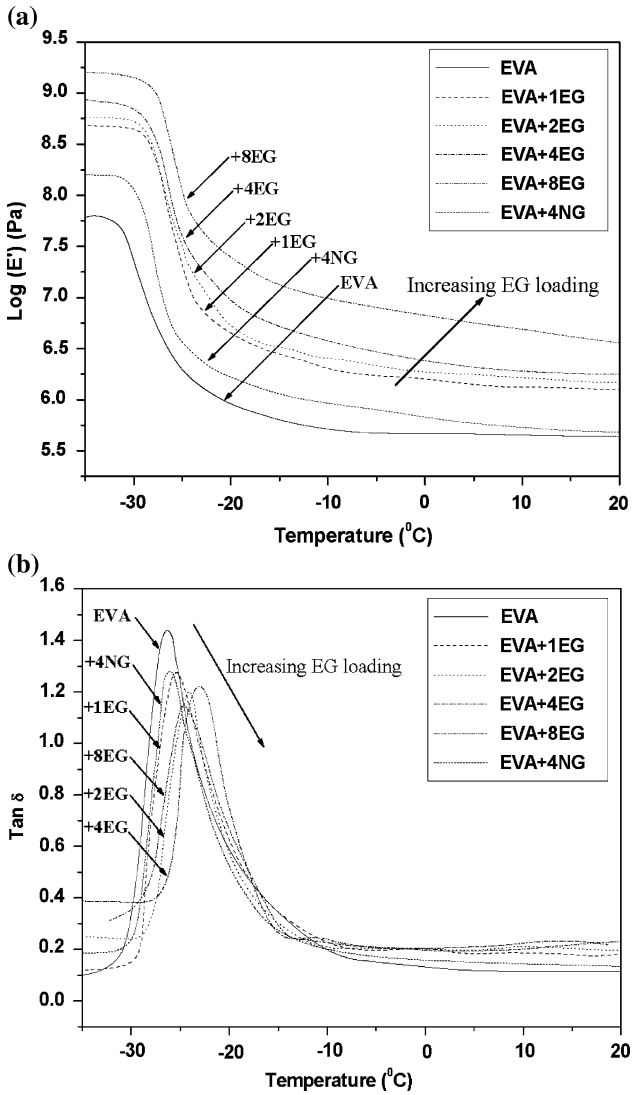

Fig. 4 Dynamic mechanical analysis for the virgin EVA and EVA + EG nanocomposites along with that of EVA + 4NG (**a**) Storage modulus versus temperature (**b**) Tan δ versus temperature

Vr_0/Vr_f is plotted against $\phi/1-\phi$ in Fig. 5. Vr_0/Vr_f decreases with $\phi/1-\phi$ in the initial stage. The slope of the Kraus plot is considered to represent the reinforcing behaviour of the filler in the matrix. The slope will be a

Table 3 Storage modulus and tan δ values at different temperatures and T_g of the nanocomposites with varying graphite loadings

Sample	Tg (°C)	Storage modulus (MPa)		Tan δ	
		At Tg	At 20 °C	At Tg	At 20 °C
EVA	–26.5	6.5	5.64	1.45	0.11
EVA + 1EG	–25.5	7.5	6.10	1.26	0.17
EVA + 2EG	–24.0	7.3	6.16	1.20	0.20
EVA + 4EG	–23.5	7.4	6.24	1.19	0.22
EVA + 8EG	–24.5	7.8	6.55	1.14	0.23
EVA + 4NG	–26.0	6.7	5.70	1.27	0.13

Table 4 Solvent swelling data of EVA + EG nanocomposites along with that of EVA + 4NG

Sample	Volume fraction of rubber
EVA	0.114 ± .002
EVA + 1EG	0.118 ± .003
EVA + 2EG	0.123 ± .003
EVA + 4EG	0.129 ± .002
EVA + 8EG	0.131 ± .003
EVA + 4NG	0.116 ± .004

direct measure of the reinforcing ability of the filler used. The greater the reinforcing ability of the filler, the more will be the swelling resistance caused by that filler. The higher negative values indicate higher interaction between the filler and the polymer. The higher value for EG sample shows that there is a significant interaction between the expanded graphite platelets and the rubber molecules.

Addition of expanded graphite provides better thermal conductivity as compared to NG filled EVA (Fig. 6). This attributes to the very well dispersed EG particles within the rubber matrix making an easy, thermally conductive network within the matrix. Incorporation of 4 phr of EG could raise the thermal conductivity of the virgin polymer from 0.24 W/mK to 0.87 W/mK.

Figure 7a–b demonstrates the TGA and DTG plots of the virgin EVA and its nanocomposites along with that of EVA-NG (4 phr) composite, carried out under nitrogen. Virgin EVA shows two-stage degradation due to the degradation of side chains (loss of acetic acid) and main chains respectively [25, 26]. Addition of EG to EVA does not change the nature of degradation, as observed from the TGA plots in Fig. 7a, but alters the temperature for

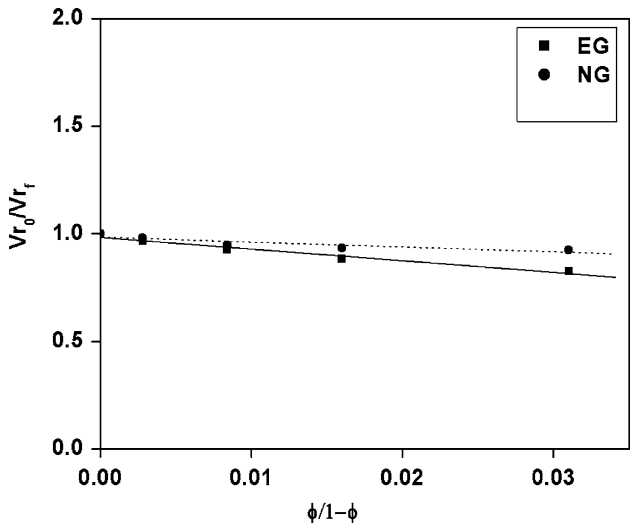

Fig. 5 Kraus plots of EVA + EG and EVA + NG

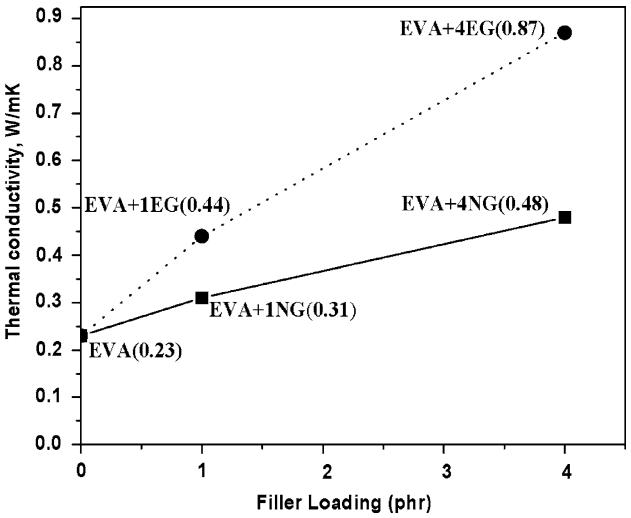

Fig. 6 Thermal conductivity of EVA + EG and EVA + NG

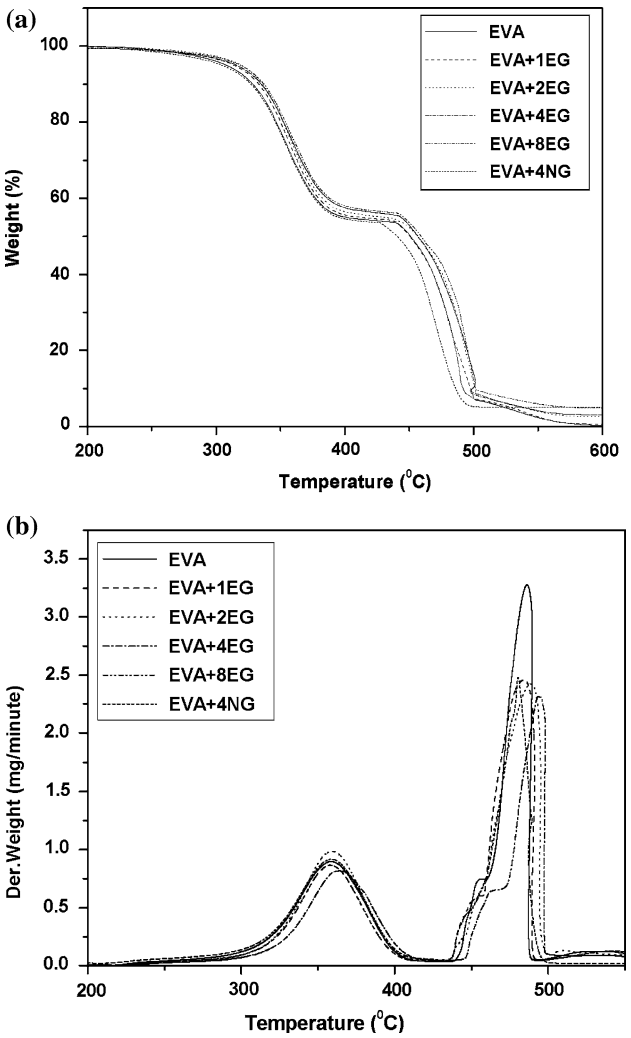

Fig. 7 Thermo-oxidative degradation plots for EVA and EVA + EG along with that of EVA + 4NG. (**a**) TGA and (**b**) DTG

Table 5 TGA and DTG data of the EVA + EG nanocomposites and EVA + 4NG

Sample	Temperature of maximum degradation, (°C)	Maximum rate of degradation mg/min)	Residue at 600 °C (%)
EVA	483	3.27	0.10
EVA + 1EG	484	2.45	0.85
EVA + 2EG	488	2.42	2.20
EVA + 4EG	498	2.31	3.10
EVA + 8EG	494	2.61	4.80
EVA + 4NG	486	2.47	4.74

maximum degradation (Table 5). A maximum shift of 14° was observed for 4 phr EG addition. Finer dispersion of EG could act as "efficient heat sinks," which consumes more heat than the matrix and does not allow the accumulation of heat within the latter, and thereby prevents oxidation at the early stages of degradation. But with 8 phr this does not improve much, rather exhibits a slight decrement. This may be due to the agglomeration of the graphite platelets within the matrix and the resulting poorer interaction. The rate of degradation in the second phase, which is observed in the principal degradation range (from 450 °C to 550 °C) of EVA is significantly improved with the incorporation of EG in the rubber matrix (Fig. 6b, the DTG plots) in comparison to the first phase of degradation (from 300 °C to 400 °C). The peak heights of the DTG plots at the higher temperature range (second phase degradation) are dropped noticeably with addition of EG, due to the same reasons stated earlier. The NG filled composite displayed poor thermal stability due to its poor dispersion and the resulting agglomerations inside the rubber phase.

Conclusions

Ethylene vinyl acetate/expanded graphite nanocomposites were prepared by solution intercalation technique followed by compression moulding, and the resulting nanocomposite properties were compared with those of NG filled EVA composite. TEM pictures revealed that the graphite platelets were homogeneously distributed in the EVA matrix, whereas the NG particles formed agglomerates inside the rubber matrix. With a loading of 4 wt% expanded graphite in EVA, the maximum tensile strength and the modulus improved over the neat EVA film by ~35 and 150% respectively. But at a higher loading of 8 wt%, the tensile strength and elongation at break exhibited significant decrement, which may be due to the relative agglomeration of the graphite particles within the matrix. The incorporation of expanded graphite provided tremendous improvement in thermal conductivity and thermal degradation resistance. A maximum shift of 14 °C in maximum rate of degradation was observed for 4 phr EG addition. This work probably paves the path for preparing stronger, light weight EVA based nanocomposites, which are cheaper than those based on carbon nanotubes, for use as advanced composites. The presence of NG adversely affected most of the properties of EVA.

References

1. Ray SS, Okamoto M (2003) Prog Polym Sci 28:1539
2. Krishnamoorti R, Vaia RA (2001) Polymer nanocopmposites, synthesis, characterization and modeling. ACS symposium series, American Chemical Society, Washington DC
3. Wen J, Wilkes GL (1996) Chem Mater 8:1667
4. Mark JE (1996) Polym Eng Sci 36:2905
5. Jain S, Goossens H, Duin M, Lemstra P (2000) Polymer 46:8805
6. Bandyopadhyay A, Bhowmick AK, Sarkar MD (2004) J Appl Polym Sci 93:2579
7. Bandyopadhyay A, Sarkar MD, Bhowmick AK (2004) Rubber Chem Technol 77:830
8. Sadhu S, Bhowmick AK (2003) Rubber Chem Technol 76:860
9. Sadhu S, Bhowmick AK (2004) J Polym Sci Polym Phy 42:1573
10. Maiti M, Sadhu S, Bhowmick AK (2004) J Polym Sci Part B Polym Phy 42:4489
11. Sengupta R, Ganguly A, Sabharwal S, Chaki TK, Bhowmick AK (2006) J Mater Sci 42:923
12. George JJ, Bandyopadhyay A, Bhowmick AK (2007) J Appl Polym Sci, doi: 10.1002/app.25067
13. Dresselhaus MS (1988) Graphite fibers and filaments. Springer-verlag, London
14. Uhl FM, Yao Q, Nakajima H, Manias E, Wilkie CA (2005) Polym Degrad Stab 89:70
15. Chung DDL (1987) J Mater Sci 22:4190
16. Uhl FM, Wilkie CA (2002) Polym Degrad Stab 76:111
17. Ping WW, Yuan PC (2004) Polym Eng Sci 44:2335
18. Xu J, Hu Y, Song L, Wang Q, Fan W, Liao G, Chen Z (2001) Polym Degrad Stab 73:29
19. Cullity BD (1978) Elements of X-ray diffraction. Addison Wesley
20. Alexander LE (1969) X-ray diffraction methods in polymer science. John Wiley, New York
21. Sadhu S, Bhowmick AK (2004) J Polymer Sci Part B Polymer Phys 42:1573
22. Zheng G, Wu J, Wang W, Pan C (2004) Carbon 42:2839
23. Yasmin A, Luo JJ, Daniel IM (2006) Composites Sci Technol 66:1182
24. Thavamani P, Bhowmick AK (1992) J Mater Sci 27:3243
25. Cai XE, Shen H (1999) J Thermal Anal Calorim 55:67
26. Costache MC, Jiang DD, Wilkie CA (2005) Polymer 46:6947